Mai, Lukas; Giedraityte, Zivile; Schmidt, Marcel; Rogalla, Detlef; Scholz, Sven; Wieck, Andreas D.; Devi, Anjana; Karppinen, Maarit

Atomic/molecular layer deposition of hybrid inorganic–organic thin films from erbium guanidinate precursor

Published in:
Journal of Materials Science

DOI:
10.1007/s10853-017-0855-6

Published: 01/06/2017

Document Version
Peer-reviewed accepted author manuscript, also known as Final accepted manuscript or Post-print

Atomic/molecular layer deposition of hybrid inorganic-organic thin films from erbium guanidinate precursor

Lukas Mai[1], Zivile Giedraityte[2], Marcel Schmidt[3], Detlef Rogalla[4], Sven Scholz[3], Andreas D. Wieck[3], Anjana Devi[1*], Maarit Karppinen[2*]

1 Inorganic Materials Chemistry, Ruhr-University Bochum, 44801 Bochum, Germany

2 Laboratory of Inorganic Chemistry, Department of Chemistry, Aalto University, P.O. Box 16100, FI-00076 Aalto, Espoo, Finland

3 Applied Solid-State Physics, Ruhr-University Bochum, 44801 Bochum, Germany

4 RUBION, Ruhr-University Bochum, 44801 Bochum, Germany

* Corresponding Authors: Anjana Devi (+49-234-32-24150),

Maarit Karppinen (+358-50-384-1726)

E-Mail addresses: lukas.mai@rub.de, zivile.giedraityte@aalto.fi, marcel.schmidt-a3k@rub.de, detlef.rogalla@rub.de, sven.scholz@rub.de, andreas.wieck@rub.de, anjana.devi@rub.de, maarit.karppinen@aalto.fi

Abstract

Luminescent erbium-based inorganic-organic hybrid materials play an important role in many frontier nano-sized applications, such as amplifiers, detectors and OLEDs. Here, we demonstrate the possibility to fabricate high-quality thin films comprising both erbium and an appropriate organic molecule as a luminescence sensitizer utilizing the combined atomic layer deposition and molecular layer deposition (ALD/MLD) technique. We employ tris(N,N'-diisopropyl-2-dimethylamido guanidinato)erbium(III) [$Er(DPDMG)_3$] together with 3,5-pyridine dicarboxylic acid (3,5-PDA) as precursors. With the appreciably high film deposition rate achieved (6.4 Å/cycle), the guanidinate precursor indeed appears as an interesting new addition to the ALD/MLD precursor variety towards novel materials. Our erbium-organic thin films showed highly promising UV absorption properties and a photoluminescence at 1535 nm for a 325 nm excitation, relevant to possible future luminescence applications.

1. Introduction

Artificial light is an indispensable part of our modern society. Especially for telecommunication, photoactive optical materials are needed to emit, transfer, amplify and detect electromagnetic radiation of the desired wavelengths. Lanthanides, more precisely the trivalent lanthanide ions, are well known for their sharp characteristic photoemission in the visible and infrared regions. [1–4] In particular, Er^{3+} with its specific emission at ~1500 nm is used as a dopant in optical silica fiber amplifiers to overcome their loss window of infrared wavelengths.[5–11] In fact, however, the absorption coefficient of Er^{3+} ions is too low for practical utilization. Sensitizing the Er^{3+} emission by complexation with strongly light-absorbing organic antenna ligands, *e.g.* aromatic molecules, capable in transferring the absorbed energy to the metal ion, offers the possibility to enhance the luminescence.[12–21] The implementation of such complexes or hybrid materials in modern applications such as organic light emitting diodes (OLED) or detectors is challenging with respect to the ever shrinking device size, and the need for flexibility and complex geometries. Furthermore, the fact that the lanthanide resources are continuously diminishing necessitates improved efficiency in the use of these elements and the performance of devices based on these elements.

Atomic layer deposition (ALD) is a state-of-the-art and industry accessible fabrication technique for high-quality, uniform and dense thin films with a well-defined composition and excellent step coverage over a multitude of different surface geometries. It is based on sequential self-limiting surface reactions applied in a cyclic manner resulting in the typical ALD film characteristics such as saturation behavior of the reactants on the surface and the linear dependency of the film thickness on the number of deposition cycles within a so-called ALD temperature window.[22, 23] Thin films grown by this technique are usually inorganic compounds such as metal oxides and nitrides. The material scope can be extended to organics though, using the related molecular layer deposition (MLD) technique based on purely organic precursors.[24, 25] Importantly, by combining inorganic ALD cycles with organic MLD cycles, meaning that an organic precursor is used as a co-reactant with the inorganic one separated by inert gas purging, it is possible to grow inorganic-organic hybrid materials, exhibiting properties derived from both the parental constituents.[26–31] One major issue regarding the combined ALD/MLD processes is the choice of suitable precursors. In order to avoid precursor condensation or gas phase decomposition it is crucial to find a combination of inorganic and organic precursors which have similar thermal properties in terms of sublimation and deposition temperatures. Furthermore, the reactivity towards each other must

be ensured. In the case of erbium, only few precursors, *e.g.* β-diketonates [Er(THD)$_3$],[32] cyclopentadienyls [Er(MeCp)$_3$][33] and amidinates [Er((^{t}BuNC(CH$_3$)N^{t}Bu)$_3$],[34] have been employed for ALD processes in literature, but drawbacks such as low reactivity, missing ALD self-limiting behavior or high impurity content in the film have been reported. In 2013, we reported a new Er-precursor, namely tris(N,N'-diisopropyl-2-dimethylamido guanidinato)erbium(III) or [Er(DPDMG)$_3$], and its successful application in a water-assisted thermal ALD process yielding stoichiometric erbium oxide thin films.[35] The advantage of this metal complex as an ALD precursor is its all-nitrogen coordinated structure, making it more reactive than other precursors while the thermal stability is maintained. With these features, the [Er(DPDMG)$_3$] complex should also be a promising candidate for ALD/MLD processes to be combined with an appropriate oxygen-containing organic precursor. Here, we select 3,5-pyridinedicarboxylic acid or 3,5-PDA for the organic precursor, as we recently demonstrated its excellent function as an efficient sensitizer for the photoluminescence of europium.[36] In this work, we present the successful ALD/MLD growth of erbium-3,5-pyridinedicarboxylate hybrid thin films based on self-limiting surface reactions of [Er(DPDMG)$_3$] and 3,5-PDA precursors (Fig. 1). The new ALD/MLD process yields high-quality thin films with appreciably high growth rates. Moreover, demonstrated are promising UV-vis absorption and photoluminescence characteristics for the films highly relevant to their possible optical applications.

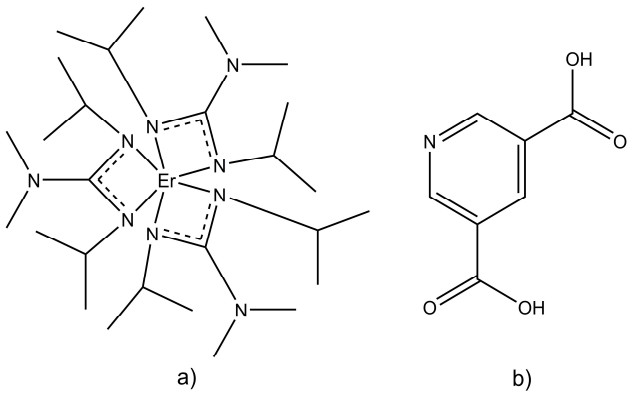

Fig. 1 Structures of the precursors: a) [Er(DPDMG)3] and b) 3,5-PDA.

Experimental Details

The erbium precursor [Er(DPDMG)$_3$] was prepared and analyzed as reported elsewhere while the synthesis was scaled-up to 10 g per batch for the ALD process development.[37] [Er(THD)$_3$] was synthesized as described in literature.[38] The organic precursor 3,5-PDA (TCI Europe N.V. purity: 98 %) was used as received without further purification. The hybrid

thin films were deposited in a commercial ALD reactor (F-120 by ASM Microchemistry Ltd.). The Si (100) substrates were rinsed with acetone and ethanol and dried in a nitrogen flow. During depositions, the precursor powders were kept in glass crucibles inside the reactor at 130 °C and 235 °C, respectively.[35, 36] Nitrogen (>99.999 %; Schmidilin UHPN 3000 N_2 generator) was used as a carrier and purging gas and a pressure of 2-4 mbar was maintained in the reactor during the film deposition. In most of the depositions the following precursor pulse / purge cycle was applied: 3 s [$Er(DPDMG)_3$] or [$Er(THD)_3$] / 5 s N_2 / 3 s 3,5-PDA / 6 s N_2. The thin films with this [$Er(DPDMG)_3$] + 3,5-PDA process were deposited within the temperature range 245 – 280 °C on Si (100) substrates.

Thickness, density and roughness of the films were determined by X-ray reflectivity (XRR; Panalytical X'Pert MPD Pro Alfa 1) measurements using XPERT HighScore Plus-reflectivity software for calculations. Grazing incidence X-ray diffraction (GIXRD) measurements with the same instrument were performed to investigate the crystallinity of the samples. Rutherford backscattering spectrometry (RBS) and nuclear reaction analysis (NRA) were carried out at RUBION Dynamitron tandem laboratories to determine the film composition in terms of C, N, O and Er. For RBS, a 2.0 MeV $^4He^+$ ion beam with an intensity of 20 - 40 nA was directed to the sample in an angle of 7 ° and scattered particles were detected by a Si detector with a resolution of 16keV at 160 °. The concentration of elements of low atomic numbers, such as C, N and O, was determined by NRA using a 1.0 MeV deuteron beam to induce nuclear reactions with the light elements. The resulting emitted protons were detected at 135 °. The detector was shielded by a 6 µm Ni-foil, to avoid scattered deuterons to be detected. SimNRA program was used to calculate the concentrations of the thin film elements by combination of RBS and NRA measurements.[39] The organic content was also verified using Fourier transform infrared spectroscopy (FTIR; Nicolet Magna-IR Spectrometer 750), where an average of 32 scans with 4 cm^{-1} resolution was applied for each sample. UV-Visible absorption spectroscopy (Perkin Elmer Lambda 950 UV/Vis/NIR absorption spectrophotometer) was used for absorbance measurements. Photoluminescence measurements were performed at the chair for applied solid state physics of the Ruhr-University Bochum to investigate the emission spectra of Er in the structure. The samples were cooled down to a temperature of T=77 K in a cryostat under vacuum condition and excited by a He-Cd laser (IK3351R-G by Kimmon Electric Co., Ltd.) with a wavelength of 325 nm and a power of 200 mW. The spectra were taken with a NIRQuest512-1.7 line-detector spectrometer in which the InGaAs-pixel were Peltier-cooled to -10 °C and operated with an integration time of 30 s.

Results and Discussion

The compatibility of the precursors is one of the substantive issues which needs to be addressed when developing a new ALD/MLD process. In particular, it is crucially important that the sublimation temperatures of the inorganic and organic sources are close enough. Another prerequisite is that the mutual reactivity of the precursors is high enough at the deposition temperature. For the reactivity, we first tested in our preliminary experiments the conventional erbium precursor [$Er(THD)_3$] in combination with 3,5-PDA for the growth of erbium(III)-di-3,5-pyridinecarboxylate [$Er_2(3,5\text{-}PDC)_3$]thin films: this process yielded a growth-per-cycle (GPC) value of 2.4 Å/cycle at 250 °C, in line with the values previously achieved for our Eu-based [$Eu(THD)_3$] + 3,5-PDA process.[36] Then, switching to the [$Er(DPDMG)_3$] precursor immediately led to a GPC value of 6.4 Å/cycle at the same deposition temperature (Fig. 2c). We ascribe this drastically increased growth rate to the high reactivity of the six Er-N bonds in [$Er(DPDMG)_3$], which are missing in [$Er(THD)_3$], towards the OH functionalities in the organic precursor.

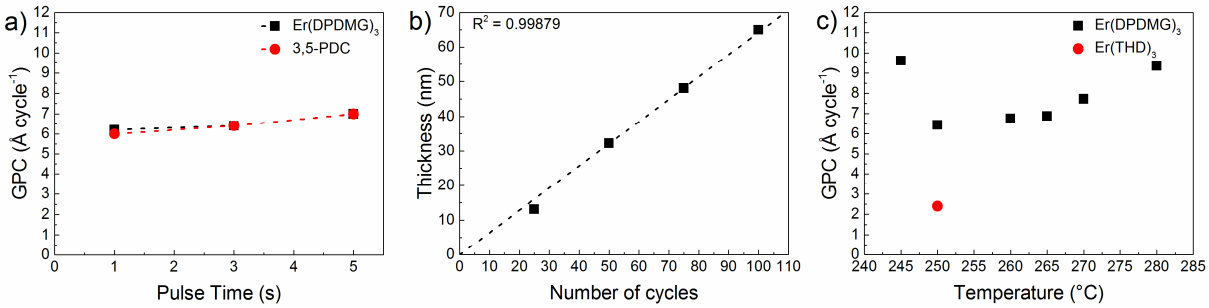

Fig. 2 ALD/MLD characteristics for the [$Er(DPDMG)_3$] / 3,5-PDA process: a) saturation study of inorganic and organic precursor; b) Linearity behavior of thickness vs number of cycles; c) Temperature dependency.

Motivated by the higher GPC values, we then further investigated and optimized the [$Er(DPDMG)_3$] + 3,5-PDA process in terms of typical ALD characteristics (Fig. 2). For the self-saturation of the precursor surface reactions, the pulse lengths of [$Er(DPDMG)_3$] and 3,5-PDA were varied between one and five seconds; for these experiments the deposition temperature was fixed at 250 °C. From Fig. 2a it can be seen that the GPC (6-7 Å $cycle^{-1}$) is not affected by the increased pulse time, indicating a saturated surface already for the 3 s precursor dose. In Fig. 2b we plot the thickness of the films against the number of ALD/MLD cycles, and as indicated by the linear fit and the corresponding R^2-value, a linear film growth is proven with a constant GPC of 6.4 Å $cycle^{-1}$ at 250 °C which, together with the surface saturation, is a strong evidence for a self-limiting behavior according to the ideal ALD/MLD

mechanism. While the so-called ALD temperature window is rarely found for ALD/MLD processes, Fig. 2c shows an essentially constant GPC in the narrow deposition temperature range of 250 – 265 °C. At temperatures higher than 270 °C, [Er(DPDMG)$_3$] starts to decompose in the gas phase and GPC is increased due to a loss of self-limiting behavior and parasitic CVD-like growth. For 245 °C, a steep rise of GPC is observed which can be explained either by precursor condensation or other three-dimensional hybrid thin film structures or polymorphs forming at these temperatures. From XRR measurements (shown in SI) we determined – besides the film thicknesses discussed above – the density and roughness values for the films. Density was found to be 2.3 g cm^{-3} and the film roughness in the order of 0.7 nm. The possible crystallinity of the films was investigated by GI-XRD measurements; the films were concluded to be essentially amorphous, as no reflections were seen in the measured GI-XRD patterns (SI, Figure S3). From the RBS spectra shown in Fig. 3, erbium, oxygen and carbon are present in all films, irrespective of the deposition temperature. The elemental concentrations determined from RBS (Er) and NRA (C, N, O) are listed in Table 1.

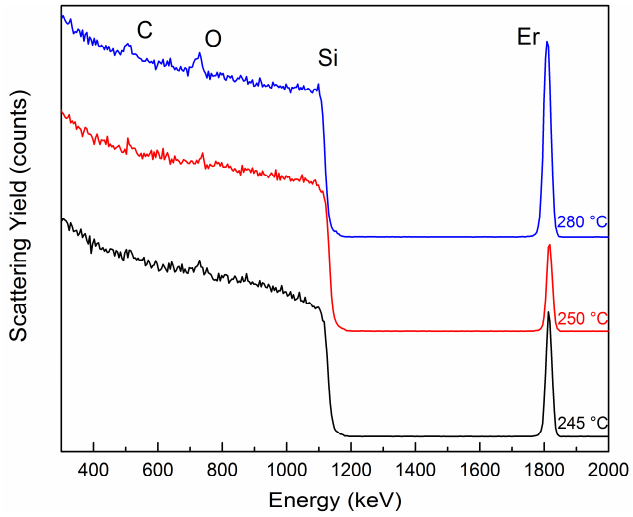

Fig. 3 RBS spectra of Er-3,5-PDC thin films grown at 245, 250 and 280 °C.

Table 1 Concentrations of C, N, O and Er in atomic% in Er-3,5-PDC hybrid thin films for different deposition temperatures.

Deposition Temperature (°C)	Atomic % (± error%)[a]			
	C	N	O	Er
Ideal concentration	55.3	7.9	31.6	5.3
245	51.3 (±3.8)	7.9 (±2.5)	35.6 (±3.4)	5.2 (±0.5)
250	51.2 (±4.7)	10.7 (±3.4)	32.6 (±4.0)	5.5 (±0.6)
280	50.8 (±3.3)	5.0 (±1.6)	38.0 (±3.0)	6.1 (±0.5)

[a] Statistical and systematic errors which belongs to the determined areal densities of atoms were calculated and Gaussian error propagation give a total error for concentrations in atomic%.

For the films deposited at 245 - 250 °C, the values are in agreement with the ideal concentrations and deviations are within the error areas of the RBS/NRA analysis, yielding in nearly stoichiometric [Er_2(3,5-PDC)$_3$] thin films. For 280 °C, the Er and O contents are slightly higher, whereas those of C and N are lower when compared with ideal values. This could be due to gas phase precipitation of the inorganic precursor and the aforementioned CVD-like process, or could arise from reactions of the film with the high energetic ion beams causing changes in concentrations.

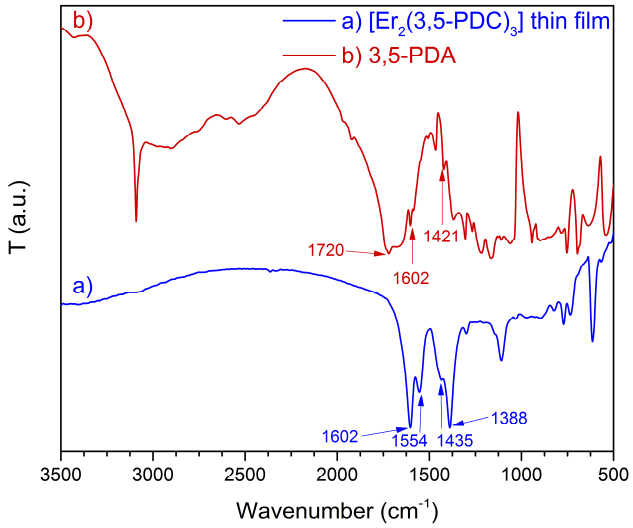

Fig. 4 FTIR spectra for 3,5-PDA and Er hybrid thin film grown at 250 °C on quartz-glass.

Table 2 Vibrational bands seen in FTIR spectra for the [Er_2(3,5-PDC)$_3$] hybrid thin film and the 3,5-PDA precursor.

Sample	ν(C=O) (cm^{-1})	ν_s(COO^-) (cm^{-1})	ν_{as}(COO^-) (cm^{-1})	ν(C=C) ring stretch (cm^{-1})	ν(C=N) ring stretch (cm^{-1})
3,5-PDA	1720	-	-	1602	1421
[Er_2(3,5-PDC)$_3$] film	-	1388	1554	1602	1435

In Fig. 4, we show the FTIR spectrum for our hybrid thin film grown from [Er(DPDMG)$_3$] and 3,5-PDA on quartz-glass and also for the 3,5-PDA precursor for reference; the spectra confirm the presence of the organic molecules and their contribution towards the thin film formation. The characteristic absorption bands seen in the spectra are summarized in Table 2. First, the characteristic bands for symmetric ν_s(COO^-) and asymmetric ν_{as}(COO^-) stretching vibrations are observed at 1388 cm^{-1} and 1554 cm^{-1}, respectively, confirming the presence of the carboxylate species. Second, the absence of the carbonyl vibration ν(C=O) at 1720 cm^{-1} and the hydroxyl stretching vibration ν(O-H) at ~3000 cm^{-1} (characteristic for carboxylic acids) confirms that the intended deprotonation reaction has taken place between the organic source 3,5-PDA and the metal precursor [Er(DPDMG)$_3$] to form the [Er_2(3,5-PDC)$_3$] moiety. A shift of the ν(C=N) ring stretching band to higher wavenumbers, *i.e.* from ca. 1421 cm^{-1} for the 3,5-PDA precursor to 1435 cm^{-1} for Er_2(3,5-PDC)$_3$ can be seen. Together with the fact that the ring stretch vibration ν(C=C) at 1602 cm^{-1} is not shifted, can be interpreted as an indication of the pyridine-N-coordination to the Er^{3+} cation in the hybrid film.[40–42]

In Fig. 5 we display normalized UV-Vis spectra for both our hybrid thin film and the 3,5-PDA precursor. In the spectrum for the 3,5-PDA precursor, the broad absorption band due to the HOMO to LUMO (n® p*) transition at 266 nm is visible. [43] In the spectrum for the deposited hybrid thin film, this band is also present but slightly shifted to 270 nm. The reason for this shift might be that the acid groups in 3,5-PDA are able to cause dimerization within the structure, which is not possible between the deprotonated carboxylate groups in the thin film and thus, result in a changed electron state environment and different absorption peak position.[44] Most importantly, the presence of the intense absorption peak at 270 nm suggests that UV light can possibly be used to excite the Er^{3+} luminescence in our [Er_2(3,5-PDC)$_3$] thin film where the 3,5-PDC ligands apparently function as antenna absorbing the light.[45, 46] Furthermore, it should be noticed that in the spectrum of the [Er_2(3,5-PDC)$_3$]

thin film the two most intensive absorption bands for the Er^{3+} cation, excitation from ground state into the $^4G_{11/2}$ state at 378 nm and into the $^2H_{11/2}$ state at 522 nm, can be clearly identified (Fig. 5 zoomed area).[12, 44]

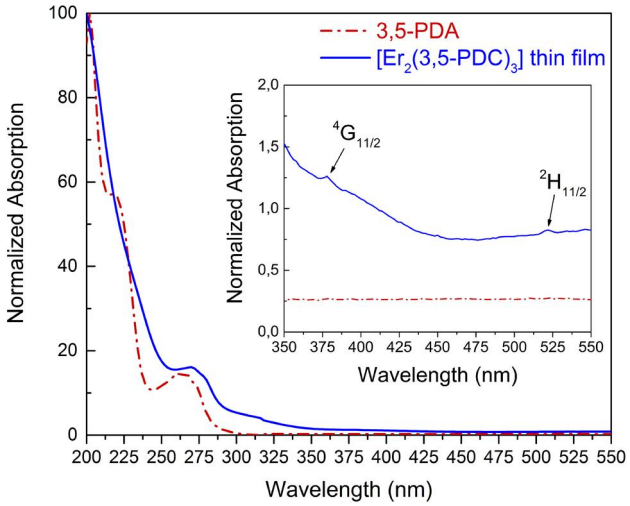

Fig. 5 UV-Vis spectra for a 45 nm $[Er_2(3,5\text{-}PDC)_3]$ hybrid thin film grown at 250 °C on quartz-glass and the pure 3,5-PDA precursor.

Finally, in order to prove the photoluminescence properties of our $Er_2(3,5\text{-}PDC)_3$ hybrid thin films we recorded an emission spectrum for the films deposited at 245 °C, 250 °C and 280 °C (Fig. 6). As excitation wavelength, 325 nm were used which correspond to a direct excitation of the Er^{3+} ions in the film. The thin films grown at 245 °C and 250 °C show a clear emission at 1535 nm which can be assigned to the transition from $^4I_{13/2}$ state into the $^4I_{15/2}$ ground state of the erbium(III) ions.[47] Interestingly, the intensity of the emission reduces with higher temperatures and at a deposition temperature of 280 °C no photoluminescence signal is detectable anymore. This is directly correlated to the amount of erbium in the samples (Table 1) and can be explained with a quenching of the photoluminescence for higher concentrations as earlier reported in the literature.[48, 49] Even if the antenna effect of the ligand could not be shown due to the lack of a suitable laser (down to 270 nm excitation) our study nicely shows that erbium hybrid structures can be used to decrease the concentration of the erbium in that amount that amplification for telecommunication wavelengths is possible.

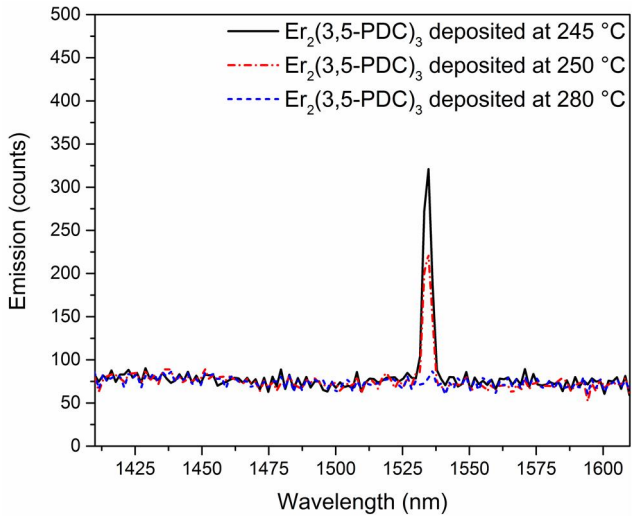

Fig. 6 Emission spectra of $Er_2(3,5\text{-}PDC)_3$ hybrid thin films grown at 245 °C, 250 °C and 280 °C, excited at 325 nm.

Conclusions

We demonstrated the excellent suitability of $[Er(DPDMG)_3]$ in combination with 3,5-PDC as precursors in ALD/MLD; in particular, appreciably high growth rates of 6.4 Å $cycle^{-1}$ were achieved. Furthermore, an ALD temperature window between 250 °C and 265 °C was confirmed within which the film thickness is linearly determined with the number of ALD/MLD cycles. Saturation studies for both the inorganic and organic precursor showed surface saturation, fulfilling the ALD/MLD criteria. With FTIR it could be shown that our inorganic precursor indeed reacts with 3,5-PDA to stoichiometric hybrid thin films of $[Er_2(3,5\text{-}PDC)_3]$; the missing carbonyl vibrations at 1720 cm^{-1} and a shift of 14 cm^{-1} of the C=N ring stretching vibration indicated the formation of Er-O and Er-N bonds within this new material. The absorption at 270 nm, which is the excitation wavelength of 3,5-PDC as an antenna, is a promising result in terms of luminescence. By direct excitation of the erbium(III) ions it was shown that an emission at 1535 nm is present wherein the intensity is highly dependent on the concentration of erbium ions.

All this shows the great advantage of using a well-developed inorganic precursor such as $[Er(DPDMG)_3]$ in combination with different organic molecules for ALD/MLD in order to produce novel materials which are precisely tailored for various applications.

Acknowledgements

The present work has received funding from the European Research Council under the European Union's Seventh Framework Programme (FP/2007-2013)/ERC Advanced Grant

Agreement (No. 339478). Furthermore, the authors at the Ruhr-University Bochum thank the DFG-SFB-TR87 and the EU-COST project HERALD for supporting this work.

References

1. Polman A, van Veggel FCJM (2004) Broadband sensitizers for erbium-doped planar optical amplifiers: Review. J. Opt. Soc. Am. B. Doi:10.1364/JOSAB.21.000871
2. Bunzli J-CG, Piguet C (2005) Taking advantage of luminescent lanthanide ions. Chem. Soc. Rev. Doi:10.1039/b406082m
3. Wang S-J, Hu J-B, Wang Y-Y, Luo F (2013) Coating graphene oxide sheets with luminescent rare-earth complexes. J Mater Sci. Doi:10.1007/s10853-012-6799-y
4. Huang X (2016) Synthesis, multicolour tuning, and emission enhancement of ultrasmall LaF3: Yb3+/Ln3+ (Ln = Er, Tm, and Ho) upconversion nanoparticles. J Mater Sci. Doi:10.1007/s10853-015-9667-8
5. Becker PC, Simpson JR, Olsson NA (1999) Erbium-doped fiber amplifiers: Fundamentals and technology. Optics and photonics. Academic Press, San Diego
6. Mears RJ, Reekie L, Jauncey IM, Payne DN (1987) Low-noise erbium-doped fibre amplifier operating at 1.54μm. Electron. Lett. Doi:10.1049/el:19870719
7. Zang Z-G, Yang W-x (2011) Theoretical and experimental investigation of all-optical switching based on cascaded LPFGs separated by an erbium-doped fiber. J. Appl. Phys. Doi:10.1063/1.3587358
8. Zang Z (2013) All-optical switching in Sagnac loop mirror containing an ytterbium-doped fiber and fiber Bragg grating. Applied optics. Doi:10.1364/AO.52.005701
9. Zang Z, Zhang Y (2012) Analysis of optical switching in a Yb3+-doped fiber Bragg grating by using self-phase modulation and cross-phase modulation. Applied optics. Doi:10.1364/AO.51.003424
10. Jha A, Shen S, Huang L, Richards B, Lousteau J (2007) Rare-earth doped glass waveguides for visible, near-IR and mid-IR lasers and amplifiers. J Mater Sci: Mater Electron. Doi:10.1007/s10854-007-9213-9
11. Kong Q, Wang J, Dong X, Yu W, Liu G (2014) Synthesis and luminescence properties of Yb3+–Er3+ co-doped LaOCl nanostructures. J Mater Sci. Doi:10.1007/s10853-013-8003-4
12. Ye HQ, Li Z, Peng Y, Wang CC, Li TY, Zheng YX, Sapelkin A, Adamopoulos G, Hernández I, Wyatt PB, Gillin WP (2014) Organo-erbium systems for optical amplification at telecommunications wavelengths. Nat. Mater. Doi:10.1038/nmat3910
13. Gillin WP, Curry RJ (1999) Erbium (III) tris(8-hydroxyquinoline) (ErQ): A potential material for silicon compatible 1.5 μm emitters. Appl. Phys. Lett. Doi:10.1063/1.123371
14. Harrison BS, Foley TJ, Bouguettaya M, Boncella JM, Reynolds JR, Schanze KS, Shim J, Holloway PH, Padmanaban G, Ramakrishnan S (2001) Near-infrared electroluminescence from conjugated polymer/lanthanide porphyrin blends. Appl. Phys. Lett. Doi:10.1063/1.1421413
15. Kang T-S, Harrison BS, Foley TJ, Knefely AS, Boncella JM, Reynolds JR, Schanze KS (2003) Near-Infrared Electroluminescence from Lanthanide Tetraphenylporphyrin: Polystyrene Blends. Adv. Mater. Doi:10.1002/adma.200304692
16. Kido J, Okamoto Y (2002) Organo Lanthanide Metal Complexes for Electroluminescent Materials. Chem. Rev. Doi:10.1021/cr010448y
17. Kuriki K, Koike Y, Okamoto Y (2002) Plastic Optical Fiber Lasers and Amplifiers Containing Lanthanide Complexes. Chem. Rev. Doi:10.1021/cr010309g
18. Nardi M, Verucchi R, Tubino R, Iannotta S (2009) Activation and control of organolanthanide synthesis by supersonic molecular beams: Erbium-porphyrin test case. Phys. Rev. B. Doi:10.1103/PhysRevB.79.125404
19. Pizzoferrato R, Lagonigro L, Ziller T, Di Carlo A, Paolesse R, Mandoj F, Ricci A, Lo Sterzo C (2004) Förster energy transfer from poly(arylene–ethynylene)s to an erbium–porphyrin complex. Chemical Physics. Doi:10.1016/j.chemphys.2004.02.006
20. Slooff LH, Polman A, Oude Wolbers MP, van Veggel FCJM, Reinhoudt DN, Hofstraat JW (1998) Optical properties of erbium-doped organic polydentate cage complexes. J. Appl. Phys. Doi:10.1063/1.366721
21. Zhao ZX, Xie TF, Li DM, Wang DJ, Liu GF (2001) Lanthanide complexes with acetylacetonate and 5,10,15,20-tetra[para-(4-flourobenzoyloxy)-meta-ethyloxy]phenylporphyrin. Synthetic Metals. Doi:10.1016/S0379-6779(00)00574-9
22. Suntola T, Antson J (1977) Method for producing compound thin films (US4058430 A)
23. Puurunen RL (2005) Surface chemistry of atomic layer deposition: A case study for the trimethylaluminum/water process. J. Appl. Phys. Doi:10.1063/1.1940727

24. Yoshimura T, Tatsuura S, Sotoyama W (1991) Polymer films formed with monolayer growth steps by molecular layer deposition. Appl. Phys. Lett. Doi:10.1063/1.105415
25. Yoshimura T, Tatsuura S, Sotoyama W, Matsuura A, Hayano T (1992) Quantum wire and dot formation by chemical vapor deposition and molecular layer deposition of one-dimensional conjugated polymer. Appl. Phys. Lett. Doi:10.1063/1.106681
26. Sundberg P, Karppinen M (2014) Organic and inorganic–organic thin film structures by molecular layer deposition: A review. Beilstein J. Nanotechnol. Doi:10.3762/bjnano.5.123
27. Dameron AA, Seghete D, Burton BB, Davidson SD, Cavanagh AS, Bertrand JA, George SM (2008) Molecular Layer Deposition of Alucone Polymer Films Using Trimethylaluminum and Ethylene Glycol. Chem. Mater. Doi:10.1021/cm7032977
28. Lee BH, Ryu MK, Choi S-Y, Lee K-H, Im S, Sung MM (2007) Rapid Vapor-Phase Fabrication of Organic−Inorganic Hybrid Superlattices with Monolayer Precision. J. Am. Chem. Soc. Doi:10.1021/ja075664o
29. Leskelä M, Ritala M, Nilsen O (2011) Novel materials by atomic layer deposition and molecular layer deposition. MRS Bull. Doi:10.1557/mrs.2011.240
30. Smirnov VM, Zemtsova EG, Belikov AA, Zheldakov IL, Morozov PE, Polyachonok OG, Aleskovskii VB (2007) Chemical design of quasi-one-dimensional organoiron nanostructures fixed on an inorganic matrix and study of their magnetic properties. Dokl Phys Chem. Doi:10.1134/S0012501607040069
31. Sood A, Sundberg P, Malm J, Karppinen M (2011) Layer-by-layer deposition of Ti–4,4′-oxydianiline hybrid thin films. Appl. Surf. Sci. Doi:10.1016/j.apsusc.2011.02.022
32. Päiväsaari J, Putkonen M, Sajavaara T, Niinistö L (2004) Atomic layer deposition of rare earth oxides: Erbium oxide thin films from β-diketonate and ozone precursors. J. Alloys Compd. Doi:10.1016/j.jallcom.2003.11.149
33. Päiväsaari J, Niinistö J, Arstila K, Kukli K, Putkonen M, Niinistö L (2005) High Growth Rate of Erbium Oxide Thin Films in Atomic Layer Deposition from (CpMe)3Er and Water Precursors. Chem. Vap. Deposition. Doi:10.1002/cvde.200506396
34. Päiväsaari J, Dezelah ICL, Back D, El-Kaderi HM, Heeg MJ, Putkonen M, Niinistö L, Winter CH (2005) Synthesis, structure and properties of volatile lanthanide complexes containing amidinate ligands: Application for Er2O3 thin film growth by atomic layer deposition. J. Mater. Chem. Doi:10.1039/b507351k
35. Xu K, Chaudhuri AR, Parala H, Schwendt D, los Arcos T de, Osten HJ, Devi A, Arcos Tdl (2013) Atomic layer deposition of Er2O3 thin films from Er tris-guanidinate and water: Process optimization, film analysis and electrical properties. J. Mater. Chem. C. Doi:10.1039/c3tc30401a
36. Giedraityte Z, Sundberg P, Karppinen M (2015) Flexible inorganic–organic thin film phosphors by ALD/MLD. J. Mater. Chem. C. Doi:10.1039/c5tc03201f
37. Milanov AP, Xu K, Cwik S, Parala H, los Arcos T de, Becker H-W, Rogalla D, Cross R, Paul S, Devi A (2012) Sc2O3, Er2O3, and Y2O3 thin films by MOCVD from volatile guanidinate class of rare-earth precursors. Dalton Trans. Doi:10.1039/c2dt31219k
38. Eisentraut KJ, Sievers RE (1965) Volatile Rare Earth Chelates. J. Am. Chem. Soc. Doi:10.1021/ja00950a051
39. Mayer M (2014) Improved physics in SIMNRA 7. Nucl. Instr. Meth. Phys. Res. B. Doi:10.1016/j.nimb.2014.02.056
40. Łyszczek R (2009) Thermal investigation and infrared evolved gas analysis of light lanthanide(III) complexes with pyridine-3,5-dicarboxylic acid. J. Anal. Appl. Pyrolysis. Doi:10.1016/j.jaap.2009.07.003
41. Ye H-M, Ren N, Zhang J-J, Sun S-J, Wang J-F (2010) Crystal structures, luminescent and thermal properties of a new series of lanthanide complexes with 4-ethylbenzoic acid. New J. Chem. Doi:10.1039/b9nj00504h
42. Puntus L, Zolin V, Kudryashova V (2004) Analysis of carboxylate coordination function of the isomeric lanthanide pyridinedicarboxylates by means of vibration spectroscopy. J. Alloys Compd. Doi:10.1016/j.jallcom.2003.11.104
43. Nataraj A, Balachandran V, Karthick T, Karabacak M, Atac A (2012) FT-Raman, FT-IR, UV spectra and DFT and ab initio calculations on monomeric and dimeric structures of 3,5-pyridinedicarboxylic acid. J. Mol. Struct. Doi:10.1016/j.molstruc.2012.05.048
44. Mech A, Monguzzi A, Meinardi F, Mezyk J, Macchi G, Tubino R (2010) Sensitized NIR Erbium(III) Emission in Confined Geometries: A New Strategy for Light Emitters in Telecom Applications. J. Am. Chem. Soc. Doi:10.1021/ja907927s
45. Puntus LN, Zolin VF, Babushkina TA, Kutuza IB (2004) Luminescence properties of isomeric and tautomeric lanthanide pyridinedicarboxylates. J. Alloys Compd. Doi:10.1016/j.jallcom.2004.03.059

46. Truillet C, Lux F, Brichart T, Lu GW, Gong QH, Perriat P, Martini M, Tillement O (2013) Energy transfer from pyridine molecules towards europium cations contained in sub 5-nm Eu2O3 nanoparticles: Can a particle be an efficient multiple donor-acceptor system? J. Appl. Phys. Doi:10.1063/1.4821428
47. Łyszczek R, Mazur L (2012) Polynuclear complexes constructed by lanthanides and pyridine-3,5-dicarboxylate ligand: Structures, thermal and luminescent properties. Polyhedron. Doi:10.1016/j.poly.2012.04.009
48. van den Hoven GN, Snoeks E, Polman A, van Dam C, van Uffelen JWM, Smit MK (1996) Upconversion in Er-implanted Al2O3 waveguides. J. Appl. Phys. Doi:10.1063/1.361020
49. Rönn J, Karvonen L, Kauppinen C, Perros AP, Peyghambarian N, Lipsanen H, Säynätjoki A, Sun Z (2016) Atomic Layer Engineering of Er-Ion Distribution in Highly Doped Er: Al 2 O 3 for Photoluminescence Enhancement. ACS Photonics. Doi:10.1021/acsphotonics.6b00283